

**Samples Preparation.** Nucleotides were extensively lyophilized and then solubilized at a final concentration of 5 mM either in a D<sub>2</sub>O solution [NaCl 100 mM, phosphate buffer 10 mM (pD 7), EDTA 0.1 mM] or in the same solution supplemented with 10 mM MgSO<sub>4</sub>. For nucleotide concentration dependence experiments, AMPPCP was first solubilized at a concentration of 50 mM and then diluted to final concentrations of 5 and 0.5 mM in the same buffer.

**NMR Measurements.** Proton spectra (90, 300, 500, and 600 MHz) were recorded on WH-90, MSL-300, WM-500, and AM-600 Bruker

spectrometers, respectively. T<sub>2</sub> and ROESY sequences were, respectively, as follows:  $\pi/2-(\tau-\pi-\tau)_n-t_2$  and  $\pi/2-t_1$ -SL- $t_2$  with a refocusing delay  $\tau$  of 1 ms and a spin-lock SL time of 300 (WM-500) or 500 ms (AM-600). All the experiments were carried out at 15 °C in order to significantly separate the residual HDO peak and the signal of the H2' ribose proton.

**Acknowledgment.** We thank Drs. P. Champeil and M. Garrigos for stimulating discussions.

## An ab Initio Study of Model S<sub>N</sub>2 Reactions with Inclusion of Electron Correlation Effects through Second-Order Møller–Plesset Perturbation Calculations

Zheng Shi and Russell J. Boyd\*

Contribution from the Department of Chemistry, Dalhousie University, Halifax, Nova Scotia, Canada B3H 4J3. Received February 20, 1990

**Abstract:** A systematic analysis of electron correlation effects in model S<sub>N</sub>2 reactions shows large differences between the structures optimized at the Hartree–Fock (HF) and second-order Møller–Plesset (MP2) levels, but the relative energies critical to an understanding of gas-phase S<sub>N</sub>2 reactions are essentially unaffected by the effect of electron correlation on the optimized structures. Integrated charges obtained from the topological definition of an atom in a molecule indicate that the HF method overestimates the ionic character at the transition state and leads to large negative charges on the nucleophiles and leaving groups. Also, the HF method underestimates the electron density at the bond critical point and overestimates the critical radius. The model systems studied are N<sup>-</sup> + CH<sub>3</sub>X → CH<sub>3</sub>N + X<sup>-</sup>, where X = H, NH<sub>2</sub>, OH, F, CCH, CN, NC, SH, and Cl for N = H and where X = H, NH<sub>2</sub>, OH, F, CN, SH, and Cl for N = F, and also N = X = Cl. The 6-31G basis set supplemented with diffuse and polarization functions (standard notation 6-31++G\*\*) was used for all atoms, except for the three methyl hydrogens for which the 6-31G basis set was used.

### Introduction

Bimolecular nucleophilic substitution (S<sub>N</sub>2) reactions at carbon are among the most extensively studied reactions of organic chemistry. While investigations of S<sub>N</sub>2 reactions have played an important role in the development of fundamental ideas in physical organic chemistry, there are major conceptual problems associated with S<sub>N</sub>2 reactions<sup>1</sup> and they continue to attract much attention from experimentalists and theoreticians.

Early theoretical studies of gas-phase S<sub>N</sub>2 reactions<sup>2</sup> provided evidence of a double-well potential energy surface and led to the proposal of a three-step mechanism of gas-phase S<sub>N</sub>2 reactions.<sup>3</sup> A systematic study<sup>4</sup> of S<sub>N</sub>2 reactions at the HF/4-31G level showed that intrinsic barriers calculated from the Marcus equation agree remarkably well with those obtained by theoretical calculation. Moreover, it also showed that there is a correlation between the geometry at the transition state (TS) and the exothermicity of the reaction. However, the basis set did not include diffuse functions, which are known to be very important for a proper

description of the electronic structures of anionic systems and for obtaining an accurate potential energy surface of a reaction involving anions.<sup>5</sup> Furthermore, electron correlation effects were not considered, and therefore there is a need to carry out higher level calculations.

Electron correlation effects on S<sub>N</sub>2 reactions have been studied by Dedieu et al. (limited configuration interaction (CI) without the Davidson correction);<sup>6</sup> by Keil and Ahlrichs (coupled electron pair approximation (CEPA));<sup>7</sup> by Černušák, Urban, and co-workers (many-body perturbation theory at the fourth order (MBPT(4)));<sup>8</sup> by Havlas et al. (second-order Møller–Plesset perturbation theory (MP2) and multiconfiguration self-consistent field theory (MCSCF));<sup>9</sup> by Vetter and Zülicke (multireference configuration interaction (MRD-CI));<sup>10</sup> and by others.<sup>11</sup> Most

(1) Brauman, J. I.; Dodd, J. A.; Han, C. C. In *Nucleophilicity*; Harris, J. M., McManus, S. P., Eds.; Advances in Chemistry Series 215; American Chemical Society: Washington, DC, 1987; p 23.

(2) (a) Dedieu, A.; Veillard, A. *Chem. Phys. Lett.* **1970**, *5*, 328. (b) Dedieu, A.; Veillard, A. *J. Am. Chem. Soc.* **1972**, *94*, 6730. (c) Dedieu, A.; Veillard, A. In *Quantum Theory of Chemical Reactions*; Daudel, R., Pullman, A., Salem, L., Veillard, A., Eds.; Reidel: Dordrecht, 1979; p 69 and references therein.

(3) (a) Olmstead, W. N.; Brauman, J. I. *J. Am. Chem. Soc.* **1977**, *99*, 4219. (b) Asubiojo, O. I.; Brauman, J. I. *Ibid.* **1979**, *101*, 3715. (c) Pellerite, M. J.; Brauman, J. I. *Ibid.* **1980**, *102*, 5993.

(4) (a) Mitchell, D. J. Ph.D. Thesis, Queen's University, Kingston, Canada, 1981. (b) Wolfe, S.; Mitchell, D. J.; Schlegel, H. B. *J. Am. Chem. Soc.* **1981**, *103*, 7692. (c) Wolfe, S.; Mitchell, D. J.; Schlegel, H. B. *Ibid.* **1981**, *103*, 7694.

(5) (a) Duke, A. J.; Bader, R. F. W. *Chem. Phys. Lett.* **1971**, *10*, 631. (b) Chandrasekhar, J.; Andrade, J. G.; Schleyer, P. v. R. *J. Am. Chem. Soc.* **1981**, *103*, 5609. (c) Clark, T.; Chandrasekhar, J.; Spitznagel, G. W.; Schleyer, P. v. R. *Comput. Chem.* **1983**, *4*, 294. (d) Hehre, W. J.; Radom, L.; Schleyer, P. v. R.; Pople, J. A. *Ab Initio Molecular Orbital Theory*; Wiley: New York, 1986. (e) Bayly, C. I.; Grein, F. *Can. J. Chem.* **1988**, *66*, 149.

(6) Dedieu, A.; Veillard, A.; Roos, B. In *Chemical and Biochemical Reactivity*; Bergmann, E. D., Pullman, B., Eds.; The Israel Academy of Sciences and Humanities: Jerusalem, 1974; p 371.

(7) Keil, F.; Ahlrichs, R. *J. Am. Chem. Soc.* **1976**, *98*, 4787. (8) (a) Černušák, I.; Urban, M.; Čársky, P.; Treindl, L. *Chem. Zvesti* **1982**, *36*, 749. (b) Urban, M.; Černušák, I.; Kellö, V. *Chem. Phys. Lett.* **1984**, *105*, 625. (c) Černušák, I.; Diercks, G. H. F.; Urban, M. *Chem. Phys. Lett.* **1986**, *128*, 538. (d) Černušák, I.; Urban, M. *Collect. Czech. Chem. Commun.* **1988**, *53*, 2239.

(9) Havlas, Z.; Merkel, A.; Kalcher, J.; Janoschek, R.; Zahradník, R. *Chem. Phys.* **1988**, *127*, 53.

(10) Vetter, R.; Zülicke, L. *J. Mol. Struct.: THEOCHEM* **1988**, *170*, 85. (11) (a) Evanseck, J. D.; Blake, J. F.; Jorgensen, W. L. *J. Am. Chem. Soc.* **1987**, *109*, 2349. (b) Shi, Z.; Boyd, R. J. *J. Am. Chem. Soc.* **1989**, *111*, 1575. (c) Tucker, S. C.; Truhlar, D. G. *J. Phys. Chem.* **1989**, *93*, 8138.

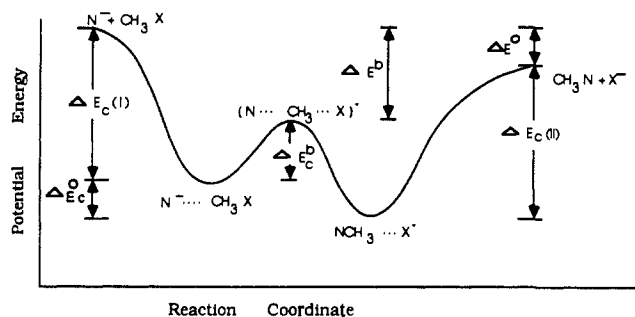


Figure 1. Schematic reaction profile of a gas-phase  $S_N2$  reaction.

of the studies were done at geometries optimized at the Hartree-Fock level. For example, Černušák et al. used the HF/4-31G geometries of Mitchell et al.<sup>8c,d</sup> and Keil and Ahlrichs used the HF/DZ+D+P geometries from Dedieu and Veillard.<sup>7</sup> Post Hartree-Fock level studies on the reaction  $H^- + CH_3F \rightarrow CH_4 + F^-$ , with geometries optimized at the MP2/6-31G\*\* level, show a pronounced dependence of the correlation energy on the geometry of the TS.<sup>9</sup> However, some uncertainty remains because the basis set did not include diffuse functions.

In this paper we present a systematic analysis of electron correlation effects for the model systems  $N^- + CH_3X \rightarrow CH_3N + X^-$ , where  $X = H, NH_2, OH, F, CCH, CN, NC, SH,$  and  $Cl$  for  $N = H$  and where  $X = H, NH_2, OH, F, CN, SH,$  and  $Cl$  for  $N = F$ , and also  $N = X = Cl$ . (In ambiguous cases the atom that bonds to carbon is italic.) The emphasis is on the optimized structures, relative energies, and electron distributions. Forthcoming papers will discuss, among other properties, the electronic structures at the TS, charge development at the TS, and intrinsic barriers.

### Computational Methods

The intent of this study is to provide qualitatively accurate results for a series of reactions with the same nucleophile. The properties of interest are not only geometries and energies but also electron densities. Thus, 6-31G extended basis sets supplemented with diffuse functions and polarization functions<sup>5c,12</sup> (standard notation 6-31++G\*\*) were used for all atoms, except the three methyl hydrogens for which the 6-31G basis set was used. In other words, diffuse and polarization functions were added to C, N (entering nucleophile), and X (leaving group). This is justified by the fact that omission of the diffuse and polarization functions on the three methyl hydrogens has only a small effect on the calculated results,<sup>2a,8b</sup> while making the computations tractable.

Second-order Møller-Plesset perturbation theory was chosen to account for the electron correlation because it has the property of being size consistent, an important requirement for the study of chemical reactivity. Two types of Møller-Plesset calculations were performed, namely single-point calculations (MP2) carried out at the geometries optimized by the HF method (MP2(full)/6-31++G\*\*//HF/6-31++G\*\*) where the keyword full indicates that inner-shell electrons are included in the treatment of electron correlation) and the optimized (MP2) calculations (MP2(full)/6-31++G\*\*//MP2(full)/6-31++G\*\*). These were done in order to study the effect of geometry on the calculated relative energies and electron distributions.

All single and double substitutions are included in the second-order Møller-Plesset calculations. Therefore, the MP2 and MP2' energies and one-electron properties are correct to the second order.

The HF, MP2', and MP2 calculations were obtained by using the GAUSSIAN 80 and GAUSSIAN 86 computer programs.<sup>13</sup> Topological properties of the electron density were calculated by using the PROAIM package and a modified PROAIM package.<sup>14</sup>

(12) Hariharan, P. C.; Pople, J. A. *Theor. Chim. Acta* **1973**, *28*, 213.

(13) (a) Binkley, J. S.; Whiteside, R. A.; Krishnan, R.; Seeger, R.; DeFrees, D. J.; Schlegel, H. B.; Topiol, S.; Kahn, L. R.; Pople, J. A. *GAUSSIAN 80*; Carnegie-Mellon Quantum Chemistry Publishing Unit: Pittsburgh, PA, 1980. (b) Frisch, M. J.; Binkley, J. S.; Schlegel, H. B.; Raghavachari, K.; Melius, C. F.; Martin, R. L.; Stewart, J. J. P.; Bobrowicz, F. W.; Rohlfing, C. M.; Kahn, L. R.; DeFrees, D. J.; Seeger, R.; Whiteside, R. A.; Fox, D. J.; Fleuder, E. M.; Pople, J. A. *GAUSSIAN 86*; Carnegie-Mellon Quantum Chemistry Publishing Unit: Pittsburgh, PA, 1984.

(14) (a) Biegler-König, F. W.; Bader, R. F. W.; Tang, T. *J. Comput. Chem.* **1982**, *3*, 317. (b) Boyd, R. J.; Wang, L. C. *J. Comput. Chem.* **1989**, *10*, 367.

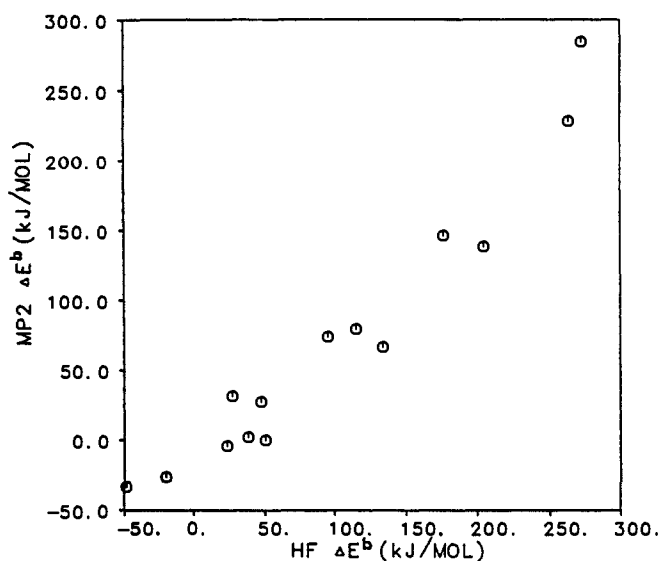


Figure 2. Comparison of  $\Delta E^b$  obtained at the HF and MP2 levels.

Geometries were optimized by use of analytical energy gradient methods at the HF and MP2 levels. Geometries of reactants, products, and transition states were fully optimized with  $C_{3v}$  or  $C_s$  symmetry constraints. Geometries corresponding to ion-molecule complexes were fully optimized with  $C_{3v}$  symmetry constraints or partially optimized with  $C_s$  symmetry constraints.<sup>15a</sup> Only backside attack is considered in this paper.<sup>15b</sup>

### Results and Discussion

A schematic plot of a gas-phase  $S_N2$  reaction profile is shown in Figure 1. According to the generally accepted mechanism proposed by Brauman et al.<sup>3</sup> the reaction involves the three steps shown by eq 1. The second step is the critical step which is responsible for the wide variation in efficiencies of  $S_N2$  reactions.<sup>3c</sup>

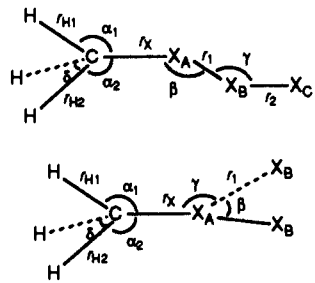


**Geometries.** Optimized geometries at the HF and MP2 levels are provided in Tables I and II. For reactants and products, the geometries optimized at the HF and MP2 levels are close to each other. For ion-molecule complexes and transition states, however, the discrepancies are large. Inclusion of electron correlation generally shortens the very loose C-N and C-X bond in  $N^- \cdots CH_3X$  and  $NCH_3 \cdots X^-$ , respectively. Electron correlation shortens the C-N and C-X bonds at the TS as well. On the other hand, the inclusion of electron correlation lengthens the C-H bonds at the TS and in the ion-molecule complexes. The changes in C-H bond lengths are far less than those observed for C-N and C-X bonds. That is, inclusion of electron correlation mainly affects the bond lengths of the relatively long (i.e., partial) bonds.

In order to investigate the effect of the choice of basis set on the optimized structures, the MP2(full)/6-31++G\*\* optimized geometries (using analytical gradients) are compared with the MP2/6-311G\*\* optimized geometries (numerical method<sup>9</sup>) in Table III for the reaction  $H^- + CH_3F \rightarrow CH_4 + F^-$ . As an aside we note that it has been shown recently that the 6-311G basis set is not of triple- $\zeta$  quality in the valence shell.<sup>16</sup> A large difference in  $r_N$  at the TS and in  $r_N$  (and  $r_X$ ) in the ion-molecule complex is observed. The MP2/6-311G\*\* calculation yields a shorter C-N bond in the TS and a shorter C-N (or C-X) bond length for the partial bonds in the ion-molecule complexes. The differences between the two methods for C-H bond lengths in the reactant, product, TS, and ion-molecule complexes, however, are small. The main difference between the two basis sets is the addition

(15) (a) For ion-molecule complexes with  $C_s$  symmetry, local minima corresponding to backside attack were found at the HF/4-31G level; see ref 4. However, they were not found at HF/6-31++G\*\* and MP2(full)6-31++G\*\* levels. (b) For the ion-molecule complexes, there are systems in which sideway attack has a lower energy (see ref 9) than backside attack. All complexes reported here correspond to backside attack.

(16) Grev, R. S.; Schaefer, H. F., III. *J. Chem. Phys.* **1989**, *91*, 7305.

Table I. Optimized Structures of  $X^-$  and  $CH_3X$  at the HF and MP2 Levels (Distances in Angstroms and Angles in Degrees)<sup>a</sup>


system	symmetry	$r_X$	$r_{H1}$	$r_{H2}$	$r_1$	$r_2$	$\alpha_1$	$\alpha_2$	$\delta$	$\beta$	$\gamma$
OH <sup>-</sup>	$C_{\infty v}$				0.948						
					0.971						
CN <sup>-</sup>	$C_{\infty v}$				1.162						
					1.201						
SH <sup>-</sup>	$C_{\infty v}$				1.338						
					1.339						
NH <sub>2</sub> <sup>-</sup>	$C_{2v}$				1.016			103.5			
					1.029			103.0			
CCH <sup>-</sup>	$C_{\infty v}$				1.233	1.060					
					1.262	1.070					
CH <sub>3</sub> H <sup>b</sup>	$T_d$	1.084									
		1.091									
CH <sub>3</sub> F	$C_{3v}$	1.371	1.081				108.5				
		1.406	1.090				108.1				
CH <sub>3</sub> Cl	$C_{3v}$	1.786	1.078				108.4				
		1.779	1.089				108.9				
CH <sub>3</sub> CN	$C_{3v}$	1.469	1.082		1.136		109.7				
		1.462	1.092		1.180		110.0				
CH <sub>3</sub> NC	$C_{3v}$	1.423	1.081		1.152		109.4				
		1.425	1.091		1.186		109.2				
CH <sub>3</sub> CCH	$C_{3v}$	1.469	1.084		1.190	1.057	110.5				
		1.462	1.094		1.221	1.063	110.7				
CH <sub>3</sub> OH	$C_s$	1.401	1.081	1.087	0.942		107.1	111.7	109.0	110.5	
		1.429	1.090	1.096	0.964		106.1	111.7	109.3	108.7	
CH <sub>3</sub> SH	$C_s$	1.818	1.082	1.081	1.328		106.8	111.2	110.0	97.9	
		1.815	1.091	1.091	1.330		106.8	111.6	109.9	96.6	
CH <sub>3</sub> NH <sub>2</sub>	$C_s$	1.453	1.090	1.084	1.000		114.5	109.2	107.4	107.8	111.6
		1.464	1.099	1.092	1.012		115.0	108.7	107.7	107.2	111.0

<sup>a</sup>In each case the MP2 value is listed immediately below the HF results. <sup>b</sup>Basis set is 6-31+G\*.

of polarization functions to the three methyl hydrogens (6-31+G\*\*) in one case, while in the other case diffuse fractions are added to N, X, and C. These results suggest that the omission of polarization functions on the methyl hydrogens is not responsible for the differences in  $r_N$  and  $r_X$ . And thus, the likely explanation for the differences in optimized geometries is the inclusion of diffuse functions. These results emphasize the importance of the choice of basis set for geometry optimizations in the study of  $S_N2$  reactions.

**Relative Energies.** Various energies shown in Figure 1 are defined in eqs 2-7.

$$\Delta E_c(I) = E(N^{\cdot-} \cdots RX) - E(N^{\cdot-} + RX) \quad (2)$$

is the energy change for the formation of the reactant ion-molecule complex from the reactants.

$$\Delta E_c(II) = E(NR \cdots X^-) - E(NR + X^-) \quad (3)$$

is the energy change for the formation of the product ion-molecule complex from the products.

$$\Delta E^b_c = E([N^{\cdot-} \cdots R \cdots X]^-) - E(N^{\cdot-} \cdots RX) \quad (4)$$

is the energy barrier for the second step of the reaction.

$$\Delta E^o_c = E(NR \cdots X^-) - E(N^{\cdot-} \cdots RX) \quad (5)$$

is the energy change for the second step of the reaction.

$$\Delta E^b = E([N^{\cdot-} \cdots R \cdots X]^-) - E(N^{\cdot-} + RX) \quad (6)$$

is the energy barrier for the entire reaction, and

$$\Delta E^o = E(NR + X^-) - E(N^{\cdot-} + RX) \quad (7)$$

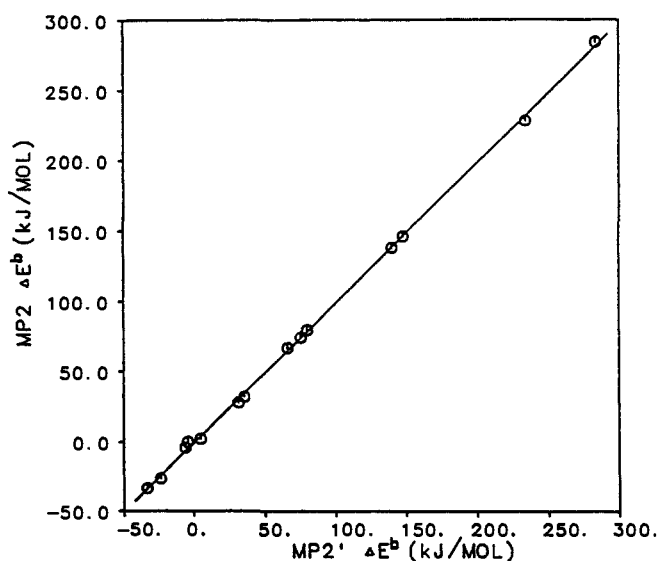
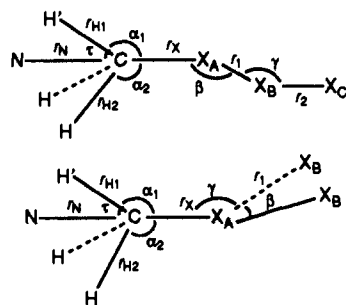


Figure 3. Comparison of  $\Delta E^b$  calculated by the MP2' and MP2 methods.

is the reaction energy of the whole reaction.

Table IV lists the various relative energies at the HF, MP2', and MP2 levels.  $\Delta E^b$  values obtained by the HF and MP2 methods are compared in Figure 2. Inclusion of electron correlation tends to reduce the energy barriers  $\Delta E^b$  (Figure 2). The MP2' and MP2 results are remarkably consistent with each other (Figure 3), despite the geometry differences. Thus, for these reactions, allowing for the effect of electron correlation on the

Table II. Optimized Structures of Ion-Molecule Complexes and Transition States at the HF and MP2 Levels (Distances in Angstroms and Angles in Degrees)<sup>a</sup>

system	symmetry	$r_N$	$r_X$	$r_{H1}$	$r_{H2}$	$r_1$	$r_2$	$\alpha_1$	$\alpha_2$	$\tau$	$D^f$	$\beta$	$\gamma$
H <sup>-</sup> ...RH	C <sub>3v</sub>	5.168	1.087	1.083				110.0					
		4.264	1.089	1.084				110.4					
(H...R...H) <sup>-</sup>	C <sub>3v</sub>	1.690	1.690	1.061				90.0					
		1.589	1.589	1.073				90.0					
H <sup>-</sup> ...RNH <sub>2</sub>	C <sub>s</sub>	4.070	1.464	1.086	1.082	1.001		114.4	109.6	65.6 <sup>b</sup>	121.3	107.1	110.7
		3.616	1.478	1.094	1.090	1.014		115.1	109.4	64.9	121.5	106.3	109.9
(H...R...NH <sub>2</sub> ) <sup>-</sup>	C <sub>s</sub>	1.738	2.029	1.062	1.062	1.012		94.5	90.1	87.5	120.3	104.4	108.6
		1.712	1.942	1.076	1.076	1.026		97.4	92.2	84.7	120.3	104.1	105.4
HR...NH <sub>2</sub> <sup>-</sup>	C <sub>s</sub>	1.090	3.792	1.082	1.082	1.016		69.2	69.3	110.8	120.1	103.3	128.3
		1.092	3.411	1.088	1.089	1.030		68.5	68.9	111.5	120.3	102.7	128.7
H <sup>-</sup> ...ROH	C <sub>s</sub>	3.619	1.420	1.078	1.082	0.942		107.5	111.7	72.5	118.8	109.2	
		3.314	1.452	1.087	1.091	0.963		106.5	111.8	73.5	118.6	107.1	
(H...R...OH) <sup>-</sup>	C <sub>s</sub>	1.791	1.890	1.062	1.062	0.946		89.9	94.3	88.1	119.6	109.7	
		1.803	1.821	1.076	1.076	0.970		92.7	97.6	85.3	119.4	104.2	
HR...OH <sup>-</sup>	C <sub>s</sub>	1.091	3.276	1.082	1.082	0.948		69.0	69.0	111.0	120.0	180.0	
		1.092	3.097	1.089	1.089	0.971		68.6	68.6	111.4	120.0	180.0	
H <sup>-</sup> ...RF	C <sub>3v</sub>	3.238	1.400	1.077				108.4					
		2.996	1.441	1.086				108.1					
(H...R...F) <sup>-1</sup>	C <sub>3v</sub>	1.874	1.764	1.062				94.4					
		1.928	1.696	1.076				98.0					
HR...F <sup>-</sup>	C <sub>3v</sub>	1.090	3.336	1.082				69.1					
		1.091	3.235	1.089				68.8					
H <sup>-</sup> ...RNC	C <sub>3v</sub>	3.159	1.445	1.077		1.150		109.8					
		2.958	1.444	1.087		1.186		110.2					
(H...R...NC) <sup>-</sup>	C <sub>3v</sub>	2.004	1.851	1.062		1.156		96.5					
		1.964	1.774	1.075		1.194		98.9					
HR...NC <sup>-</sup>	C <sub>3v</sub>	1.088	3.878	1.083		1.162		69.7					
		1.089	3.592	1.089		1.201		69.4					
H <sup>-</sup> ...RCCH	C <sub>3v</sub>	3.560	1.473	1.082		1.193	1.056	111.3					
		3.372	1.465	1.092		1.224	1.062	112.0					
(H...R...CCH) <sup>-</sup>	C <sub>3v</sub>	1.846	2.057	1.061		1.217	1.059	93.5					
		1.780	1.982	1.073		1.247	1.067	94.8					
HR...CCH <sup>-</sup>	C <sub>3v</sub>	1.088	4.390	1.083		1.233	1.060	69.7					
		1.090	4.005	1.089		1.262	1.071	69.4					
H <sup>-</sup> ...RCN	C <sub>3v</sub>	3.221	1.475	1.080		1.138		110.9					
		3.086	1.465	1.090		1.181		111.6					
(H...R...CN) <sup>-</sup>	C <sub>3v</sub>	1.909	1.996	1.062		1.151		95.1					
		1.845	1.927	1.074		1.193		96.6					
HR...CN <sup>-</sup>	C <sub>3v</sub>	1.087	4.463	1.083		1.162		69.8					
		1.089	4.035	1.089		1.201		69.6					
H <sup>-</sup> ...RSH	C <sub>s</sub>	3.474	1.832	1.079	1.078	1.328		107.3	111.5	72.7	118.5	98.5	
		3.235	1.827	1.089	1.088	1.331		107.7	112.2	72.3	118.4	97.2	
(H...R...SH) <sup>-</sup>	C <sub>s</sub>	2.029	2.253	1.064	1.063	1.332		96.1	97.9	83.4	119.5	97.3	
		1.952	2.183	1.077	1.076	1.334		98.2	100.3	81.5	119.4	94.1	
HR...SH <sup>-</sup>	C <sub>s</sub>	1.088	4.249	1.083	1.083	1.337		69.8	69.8	110.2	120.0	180.0	
		1.090	3.833	1.090	1.089	1.339		69.7	69.4	110.3	112.0	150.3	
H <sup>-</sup> ...RCl	C <sub>3v</sub>	3.086	1.834	1.073				107.9					
		2.943	1.820	1.085				108.9					
(H...R...Cl) <sup>-</sup>	C <sub>3v</sub>	2.235	2.086	1.064				100.0					
		2.152	2.027	1.078				102.5					
HR...Cl <sup>-</sup>	C <sub>3v</sub>	1.088	4.462	1.083				69.8					
		1.089	4.018	1.089				69.5					
F <sup>-</sup> ...RNH <sub>2</sub>	C <sub>s</sub>	3.043	1.472	1.083	1.080	1.002		114.7	110.0	65.3	121.3	106.7	110.4
(F...R...NH <sub>2</sub> ) <sup>-</sup>	C <sub>s</sub>	1.762	2.144	1.061	1.062	1.012		90.0	85.0	92.7	120.3	104.2	112.7
		1.710	2.178	1.076	1.076	1.026		88.4	82.0	95.1	120.4	103.7	110.7
FR...NH <sub>2</sub> <sup>-</sup>	C <sub>s</sub>	1.414	2.953	1.074	1.075	1.014		71.6	71.8	108.4	120.2	103.3	128.3
F <sup>-</sup> ...ROH	C <sub>s</sub>	2.870	1.431	1.076	1.080	0.941		107.6	111.7	72.4	118.9	108.9	
		2.812	1.462	1.085	1.089	0.963		106.7	111.8	73.3	118.6	106.9	
(F...R...OH) <sup>-</sup>	C <sub>s</sub>	1.795	1.990	1.061	1.061	0.946		84.9	89.7	97.5	119.8	112.9	
		1.760	2.008	1.075	1.075	0.969		83.1	88.7	94.1	119.7	108.2	
FR...OH <sup>-</sup>	C <sub>s</sub>	1.415	2.736	1.074	1.074	0.945		71.7	71.7	108.3	120.0	180.0	
		1.452	2.670	1.083	1.084	0.969		72.2	71.9	107.8	119.9	160.1	

Table II (Continued)

system	symmetry	$r_N$	$r_X$	$r_{HI}$	$r_{H2}$	$r_1$	$r_2$	$\alpha_1$	$\alpha_2$	$\tau$	$D^c$	$\beta$	$\gamma$
F...RF	$C_{3v}$	2.674	1.416	1.074				108.1					
		2.627	1.454	1.084				107.7					
(F...R...F) <sup>-</sup>	$C_{3v}$	1.846	1.846	1.061				90.0					
		1.836	1.836	1.074				90.0					
F...RCN	$C_{3v}$	2.722	1.477	1.079		1.140		111.3					
(F...R...CN) <sup>-</sup>	$C_{3v}$	1.882	2.072	1.062		1.152		91.1					
		1.829	2.065	1.074		1.193		89.5					
FR...CN <sup>-</sup>	$C_{3v}$	1.397	3.288	1.077		1.160		71.6					
F...RSH	$C_s$	2.804	1.842	1.077	1.075	1.329		107.5	111.5	72.6	118.6	98.9	
(F...R...SH) <sup>-</sup>	$C_s$	1.977	2.331	1.062	1.061	1.333		91.9	93.9	87.2	119.6	98.6	
		1.887	2.328	1.075	1.073	1.335		90.1	91.7	89.3	119.5	95.8	
FR...SH <sup>-</sup>	$C_s$	1.397	3.604	1.078	1.076	1.336		71.7	71.5	108.3	120.0	121.1	
F...RCl	$C_{3v}$	2.585	1.863	1.070				107.0					
		2.615	1.831	1.082				108.5					
(F...R...Cl) <sup>-</sup>	$C_{3v}$	2.126	2.133	1.062				97.3					
		2.013	2.142	1.073				95.6					
FR...Cl <sup>-</sup>	$C_{3v}$	1.398	3.422	1.077				71.6					
		1.437	3.251	1.086				72.0					
Cl...RCl	$C_{3v}$	3.367	1.824	1.073				108.0					
		3.266	1.808	1.084				108.9					
(Cl...R...Cl) <sup>-</sup>	$C_{3v}$	2.393	2.394	1.062				90.0					
		2.316	2.316	1.072				90.0					

<sup>a</sup>In each case the MP2 value is listed immediately below the HF results. Where only one set of values is listed, the MP2 results are unavailable. R = CH<sub>3</sub>. <sup>b</sup>For ion-molecule complexes with  $C_s$  symmetry, the angle is fixed so that  $\angle NCX = 180.0^\circ$ . <sup>c</sup>Dihedral angle  $D$  (H'CX<sub>A</sub>H).

Table III. Optimized Bond Lengths for the Reaction  $H^- + CH_3F \rightarrow CH_4 + F^-$  (Å)

system	method	$r_N$	$r_X$	$r_H$
CH <sub>3</sub> F	MP2 <sup>a</sup>		1.4056	1.0900
	MP2* <sup>b</sup>		1.3816	1.0917
	HF <sup>c</sup>		1.3714	1.0807
H...CH <sub>3</sub> F	MP2	2.9963	1.4407	1.0859
	MP2*	2.8359	1.4178	1.0872
	HF	3.2381	1.3997	1.0766
[H...CH <sub>3</sub> ...F] <sup>-</sup>	MP2	1.9278	1.6955	1.0759
	MP2*	1.8166	1.7060	1.0744
	HF	1.8742	1.7640	1.0622
CH <sub>3</sub> ...F <sup>-</sup>	MP2	1.0912	3.2351	1.0886
	MP2*	1.0982	2.7653	1.0850
	HF	1.0903	3.3360	1.0817
CH <sub>4</sub>	MP2			1.0905
	MP2*			1.0909
	HF			1.0840

<sup>a</sup>MP2(full)/6-31++G\*\* optimized geometries from this work, except for CH<sub>4</sub> where the 6-31HG\* basis set was used. <sup>b</sup>MP2/6-311G\*\* optimized geometries from ref 9. <sup>c</sup>Geometries optimized at the HF/6-31++G\*\* level, except for CH<sub>4</sub> in which no diffuse and polarization functions are included on hydrogens.

optimized structures has very little effect on the relative energies.

Our energy barriers  $\Delta E^b$  are compared with the results of MBPT(4) calculations<sup>8d</sup> in Table V. The MBPT(4) results are the only data available in the literature with which a comparison of relative energies for a series of reactions with the same nucleophile or leaving group can be made. The MBPT(4) calculations were carried out at the geometries optimized at the HF/4-31G level with a DZ+P+D basis set (polarization and diffuse functions were omitted for all hydrogens). The main difference between the MBPT(4) and our MP2 calculations is the choice of geometries. The former used the TS geometries optimized at the HF/4-31G level or partially optimized at the HF/DZ+P+D level,<sup>8b,d</sup> while the latter used geometries optimized at the MP2(full)/6-31++G\*\* level. Also, the order of perturbation correction differs: the former is correct to the fourth order, whereas the latter is correct to the second order. With the exception of N = CN, the MP2 barriers are lower than the MBPT(4) barriers. Nevertheless, the two methods give consistent results (see Figure 4). A recent study of the reaction  $H^- + CH_3F \rightarrow CH_4 + F^-$  shows that a  $\Delta E^b$  value of about 4.2 kJ/mol gives a rate constant that agrees closely with the experimental results.<sup>17</sup>

(17) Merkel, A.; Havlas, Z.; Zahradník, R. *J. Am. Chem. Soc.* **1988**, *110*, 8355.

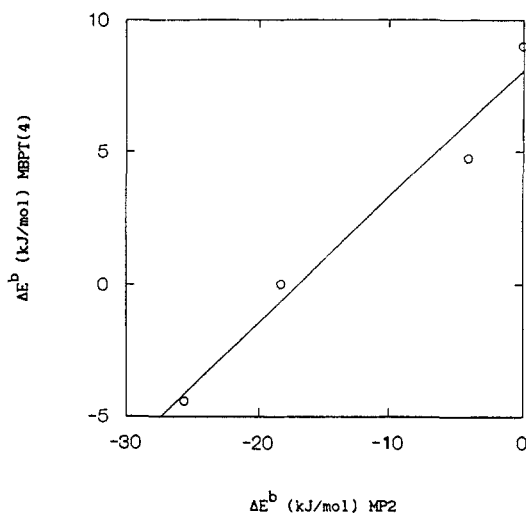


Figure 4. Comparison of  $\Delta E^b$  calculated by the MP2 and MBPT(4) methods.

This  $\Delta E^b$  value is in between the MBPT(4) and MP2 values. It should be noted that an experimental Arrhenius activation energy  $E_a = 16$  kJ/mol obtained<sup>18</sup> by use of the equation  $k_{obs} = k_{ADO} \exp(-E_a/RT)$  must be disregarded in view of the accepted interpretation of gas-phase  $S_N2$  reactions.<sup>19</sup>

**Electron Distributions.** The essential topological properties of the electron density can be summarized by the complete specification of its critical points, at which  $\nabla\rho = 0$ .<sup>20</sup> Each critical point can be classified according to its rank and signature ( $\lambda, \sigma$ ). The rank  $\lambda$  of a critical point equals the number of nonzero eigenvalues of the Hessian matrix of  $\rho(r_c)$ , while the signature  $\sigma$  is the algebraic sum of the signs of the eigenvalues. For example, a (3,-1) critical point has two negative and one positive eigenvalues. The two eigenvectors associated with the negative eigenvalues define a surface on which the critical point is a local

(18) Tanaka, K.; Mackay, G. I.; Payzant, J. D.; Bohme, D. K. *Can. J. Chem.* **1976**, *54*, 1643.

(19) Riveros, J. M.; José, S. M.; Takashima, K. *Adv. Phys. Org. Chem.* **1985**, *21*, 197.

(20) (a) Bader, R. F. W.; Tal, Y.; Anderson, S. G.; Nguyen-Dang, T. T. *Isr. J. Chem.* **1980**, *19*, 8. (b) Bader, R. F. W.; Nguyen-Dang, T. T. *Adv. Quantum Chem.* **1981**, *14*, 63. (c) Bader, R. F. W.; Nguyen-Dang, T. T.; Tal, Y. *Rep. Prog. Phys.* **1981**, *44*, 893.

Table IV. Energies Calculated at the HF, MP2', and MP2 Levels<sup>a</sup> (kJ/mol)

N <sup>-</sup> + RX	$\Delta E_c(I)$	$\Delta E_c(II)$	$\Delta E_c^b$	$\Delta E_c^c$	$\Delta E^b$	$\Delta E^c$
H <sup>-</sup> + RH <sup>b</sup>	-0.63	-0.63	264.12	0.00	263.49	0.00
	-1.53	-1.53	235.15	0.00	233.62	0.00
	-2.07	-2.07	230.86	0.00	228.78	0.00
H <sup>-</sup> + RNH <sub>2</sub>	-6.18	-2.92	210.76	-38.90	204.57	-42.16
	-10.03	-6.07	150.45	-87.92	140.42	-91.88
	-10.95	-6.88	149.48	-87.37	138.53	-91.44
H <sup>-</sup> + ROH	-15.55	-5.35	149.50	-112.05	133.95	-122.26
	-20.62	-9.23	87.14	-176.57	66.52	-187.97
	-21.39	-9.80	88.59	-174.83	67.20	-186.42
H <sup>-</sup> + RF	-31.43	-4.10	82.11	-194.73	50.67	-222.06
	-36.71	-7.00	32.93	-257.47	-3.78	-287.18
	-37.42	-7.17	37.36	-254.61	-0.06	-284.86
H <sup>-</sup> + RNC	-45.02	-1.65	83.40	-282.88	38.38	-326.35
	-55.74	-3.92	60.83	-308.41	5.09	-360.23
	-57.30	-4.32	59.48	-308.37	2.19	-361.34
H <sup>-</sup> + RCCH	-18.68	-1.39	194.88	-116.98	176.20	-134.27
	-23.93	-3.30	172.35	-127.13	148.42	-147.77
	-24.23	-3.66	170.69	-125.32	146.46	-145.90
H <sup>-</sup> + RCN	-47.14	-1.26	142.51	-200.71	95.37	-246.59
	-51.49	-2.97	127.25	-206.61	75.76	-255.13
	-51.42	-3.35	126.23	-203.48	74.81	-251.55
H <sup>-</sup> + RSH	-20.65	-1.54	68.35	-285.94	47.70	-305.05
	-24.92	-3.96	56.50	-275.57	31.58	-296.54
	-25.63	-5.61	53.65	-276.04	28.02	-296.06
H <sup>-</sup> + RCI	-36.17	-1.25	16.41	-373.94	-19.76	-408.86
	-38.53	-3.47	15.35	-364.49	-23.18	-399.55
	-39.31	-4.01	13.11	-363.79	-26.20	-399.08
F <sup>-</sup> + RH	-4.10	-31.43	276.84	194.73	272.74	222.06
	-7.00	-36.71	290.40	257.47	283.40	287.18
	-7.17	-37.42	291.98	254.61	284.80	284.86
F <sup>-</sup> + RNH <sub>2</sub>	-15.73	-50.51	210.39	145.11	194.67	179.90
	-20.92	-57.64	188.95	158.58	168.03	195.30
					167.74	193.39
F <sup>-</sup> + ROH	-30.28	-55.50	145.84	74.58	115.56	99.81
	-35.76	-60.68	115.85	74.30	80.08	99.21
	-35.96	-60.83	116.13	73.57	80.17	98.44
F <sup>-</sup> + RF	-53.74	-53.74	77.55	0.00	23.81	0.00
	-58.24	-58.24	52.70	0.00	-5.54	0.00
	-58.21	-58.21	54.09	0.00	-4.12	0.00
F <sup>-</sup> + RCN	-71.97	-32.52	143.07	14.92	71.10	-24.52
	-73.19	-37.32	153.94	67.92	80.75	32.05
					82.10	33.29
F <sup>-</sup> + RSH	-37.52	-31.19	67.01	-76.66	29.49	-82.98
	-40.34	-38.38	79.79	-7.40	39.45	-9.36
					38.49	-11.21
F <sup>-</sup> + RCI	-60.73	-33.64	12.51	-159.70	-48.22	-186.80
	-57.97	-39.31	25.13	-93.71	-32.84	-112.37
	-58.83	-39.92	25.56	-95.31	-33.27	-114.22
Cl <sup>-</sup> + RCI	-37.15	-37.15	64.72	0.00	27.57	0.00
	-39.72	-39.72	75.44	0.00	35.72	0.00
	-40.42	-40.42	72.54	0.00	32.12	0.00

<sup>a</sup>The HF energies are followed by the MP2' and MP2 energies. <sup>b</sup>To make the basis set consistent throughout the series of reactions, the calculations for methane were done first at the 6-31+G\* level and then at the 6-31++G\*\* level with diffuse and polarization functions added to all hydrogens. The energy corresponding to a basis set with polarization and diffuse functions added to carbon and one of the hydrogen atoms was obtained by extrapolation.

maximum. The eigenvector associated with the positive eigenvalue defines a unique axis along which the charge density decreases for motion toward the critical point.  $\rho(r_c)$  is the local minimum along this axis. A (3,-1) critical point appears between every pair of neighboring bonded atoms and is therefore called a bond critical point. Studies have shown that the electron density at the bond critical point is related to the bond type and bond order and that the critical radius is related to the electronegativities of the bonded atoms.<sup>21</sup> Calculated bond critical points at the TS are listed in Table VI, where  $r_{c-Y}$  is the distance between atom Y and the C-Y bond critical point and  $\rho_{c-Y}$  is the electron density at the C-Y bond critical point. In most cases the effect of including electron correlation is to increase the electron density at the bond critical point and to decrease the distance from the bond critical point to the nucleophile. The MP2' results generally lie intermediate between the HF and MP2 results. These observations can be rationalized by the fact that the HF method overestimates ionic character.<sup>22</sup> The large ionic character at the HF level makes the

electron density at the bond critical point small and the critical radius ( $r_{c-Y}$ ) longer.<sup>21</sup>

The integrated charges, obtained from the topological definition of an atom in a molecule,<sup>20</sup> on N and X at the TS are compared for the three theoretical levels discussed herein in Figures 5-7. As the HF method overestimates ionic character, it always yields large negative charges on N and X (Figure 5). The MP2' method lowers the charge on N and X similarly, as indicated by the similar correlation for the two sets of data in Figure 6 relative to Figure 5, whereas the MP2 method lowers the charge on N and X

(21) (a) Bader, R. F. W.; Tang, T.; Tal, Y.; Biegler-König, F. W. *J. Am. Chem. Soc.* **1982**, *104*, 946. (b) Wiberg, K. B.; Bader, R. F. W.; Lau, C. D. *H. Ibid.* **1987**, *109*, 985. (c) Boyd, R. J.; Edgecombe, K. E. *J. Am. Chem. Soc.* **1988**, *110*, 4182.

(22) (a) Pilar, F. *Elementary Quantum Chemistry*; McGraw-Hill: New York, 1968; pp 491, 517. (b) McWeeny, R.; Sutcliffe, B. T. *Methods of Molecular Quantum Mechanics*; Academic Press: New York, 1969; p 61. (c) Wang, L. C.; Boyd, R. J. *J. Chem. Phys.* **1989**, *90*, 1083.

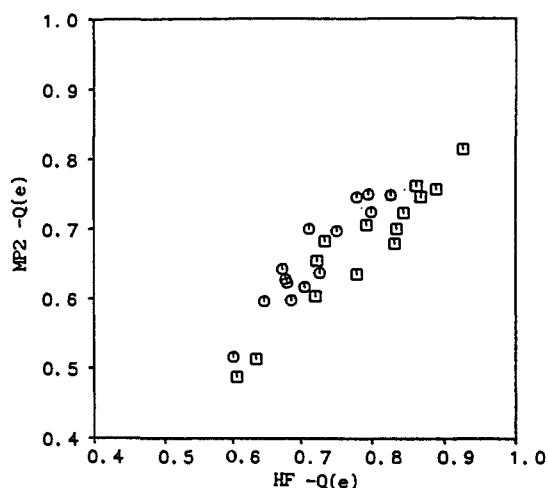


Figure 5. Comparison of integrated charges at the HF and MP2 levels:  $\square$  is the more electronegative group between N and X, and  $\circ$  indicates the less electronegative group.

Table V. Energy Barriers for the Reactions  $N^- + CH_3F \rightarrow CH_3N + F^-$  (kJ/mol)

N	$\Delta E^b$	
	MP2 <sup>a</sup>	MBPT(4) <sup>c</sup>
H	-0.06	9.01
F	-4.12	4.74
OH	-18.27	0.02
NH <sub>2</sub>	-25.65	-4.43
CN	48.81	11.89

<sup>a</sup>MP2(full)/6-31++G\*\*//MP2(full)/6-31++G\*\* data from this work. <sup>c</sup>Many-body perturbation calculation from ref 8d.

unequally. Depending on the electronegativity of N and X, MP2 lowers the charge on the more electronegative group to a larger extent than on the less electronegative group (see Figures 5 and 7).

### Conclusions

Large differences are observed in the geometries optimized by the HF and MP2 methods for ion-molecule complexes and transition states. However, the two methods yield very similar structures for reactants and products. For the reaction  $H^- + CH_3F \rightarrow CH_4 + F^-$ , the MP2(full)/6-31++G\*\* and MP2/6-31|G\*\* methods give quite different C-N bond lengths at the TS and in the ion-molecule complex and substantially different C-X bond lengths in the ion-molecule complex. This shows that the basis set has a large effect on the optimized geometries. The differences in geometries have only a small effect, however, on the calculated relative energies ( $\Delta E^b$ ,  $\Delta E^c$ ,  $\Delta E^d$ , etc.) provided the same basis

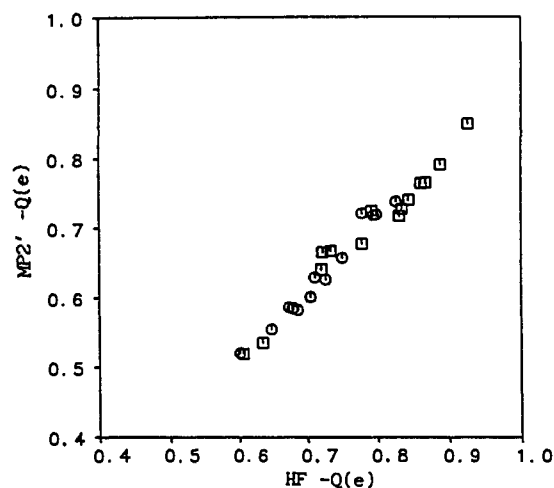


Figure 6. Comparison of integrated charges obtained at the HF and MP2' levels:  $\square$  indicates the more electronegative group between N and X, and  $\circ$  indicates the less electronegative group.

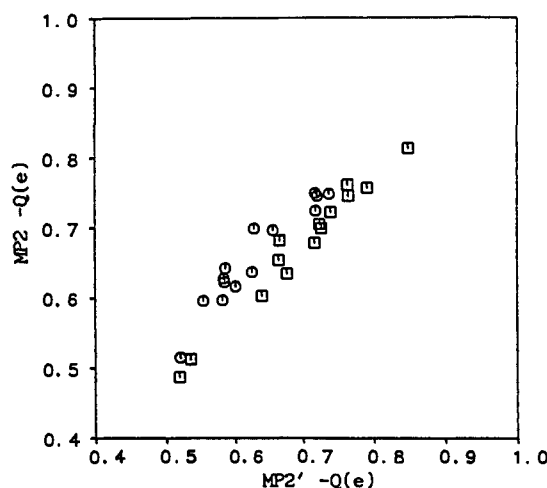


Figure 7. Comparison of integrated charges on N and X obtained at the MP2' and MP2 levels:  $\square$  indicates the more electronegative group, and  $\circ$  indicates the less electronegative group.

sets are used. This is demonstrated by the close agreement between the MP2' and MP2 results. Comparison of the energy barriers ( $\Delta E^b$ ) obtained in this work with MBPT(4) data from the literature indicates that the MP2 method usually yields a lower activation energy than the MBPT(4) method and that, with the exception of  $N = CN$ , the two methods give consistent results. The HF, MP2', and MP2 methods give different results for the

Table VI. Critical Points of Transition-State Structures at the HF, MP2', and MP2 Levels (au)

[N...R...X] <sup>-</sup>	$r_{e-N}$			$\rho_{e-N}$		
	HF	MP2'	MP2	HF	MP2'	MP2
[H...R...H] <sup>-</sup>	1.351	1.286	1.189	0.068	0.071	0.086
[H...R...NH <sub>2</sub> ] <sup>-</sup>	1.440	1.363	1.340	0.061	0.064	0.066
[H...R...OH] <sup>-</sup>	1.512	1.456	1.446	0.058	0.058	0.054
[H...R...F] <sup>-</sup>	1.608	1.533	1.592	0.045	0.048	0.042
[H...R...NC] <sup>-</sup>	1.739	1.672	1.633	0.035	0.038	0.039
[H...R...CCH] <sup>-</sup>	1.556	1.484	1.420	0.049	0.052	0.058
[H...R...CN] <sup>-</sup>	1.622	1.554	1.491	0.043	0.046	0.050
[H...R...SH] <sup>-</sup>	1.712	1.646	1.567	0.035	0.036	0.041
[H...R...Cl] <sup>-</sup>	1.941	1.883	1.793	0.023	0.024	0.027
[F...R...H] <sup>-</sup>	1.945	1.853	1.818	0.090	0.105	0.123
[F...R...NH <sub>2</sub> ] <sup>-</sup>	1.962	1.874	1.844	0.089	0.103	0.117
[F...R...OH] <sup>-</sup>	1.986	1.903	1.879	0.081	0.095	0.103
[F...R...F] <sup>-</sup>	2.019	1.943	1.937	0.071	0.084	0.086
[F...R...CN] <sup>-</sup>	2.026	1.961	1.924	0.068	0.079	0.089
[F...R...SH] <sup>-</sup>	2.080	2.015	1.948	0.056	0.065	0.079
[F...R...Cl] <sup>-</sup>	2.191	2.143	2.052	0.040	0.046	0.059
[Cl...R...Cl] <sup>-</sup>	2.657	2.571	2.494	0.043	0.047	0.055

charge distribution at the TS. The HF method overestimates the ionic character and yields large negative charges on N and X. In a later paper, we will compare the relative change in charge distribution from reactants to the TS and from the TS to the products.

**Acknowledgment.** A Killam postgraduate scholarship (to Z.S.) from Dalhousie University and the financial assistance of the Natural Sciences and Engineering Research Council of Canada in the form of an operating grant (to R.J.B.) are gratefully acknowledged. We are grateful to Dalhousie University Computing

and Information Services for a generous allocation of computer time.

**Registry No.** CH<sub>3</sub>H, 74-82-8; CH<sub>3</sub>F, 593-53-3; CH<sub>3</sub>Cl, 74-87-3; CH<sub>3</sub>CN, 75-05-8; CH<sub>3</sub>NC, 593-75-9; CH<sub>3</sub>CCH, 74-99-7; CH<sub>3</sub>OH, 67-56-1; CH<sub>3</sub>SH, 74-93-1; CH<sub>3</sub>NH<sub>2</sub>, 74-89-5; H<sup>-</sup>, 12184-88-2; F<sup>-</sup>, 16984-48-8; Cl<sup>-</sup>, 16887-00-6; OH, 14280-30-9; NH<sub>2</sub>, 17655-31-1; CN, 57-12-5.

**Supplementary Material Available:** Tables of total energies at the HF, MP2', and MP2 levels of all species described herein (2 pages). Ordering information is given on any current masthead page.

## On the Evaluation of Interproton Distances for Three-Dimensional Structure Determination by NMR Using a Relaxation Rate Matrix Analysis

Carol Beth Post,<sup>\*,†,‡</sup> Robert P. Meadows,<sup>‡</sup> and David G. Gorenstein<sup>\*,‡</sup>

Contribution from the Department of Biological Sciences and Department of Chemistry, Purdue University, West Lafayette, Indiana 47907. Received October 6, 1989

**Abstract:** The accuracy of interproton distances obtained from two-dimensional nuclear Overhauser effect (NOESY) data using a relaxation rate matrix approach is examined by theoretical simulation studies. Interproton distances, the basis for three-dimensional structure determination of macromolecules by NMR, are most often evaluated from NOESY data by using a two-spin approximation or by grouping according to strong, medium, and weak intensities. A more rigorous analysis considers interactions within the full multispin system as specified by the relaxation rate matrix. With this matrix, distances are evaluated directly from measured NOESY volumes at a single mixing time taking into account indirect relaxation effects. However, numerical errors and mathematical difficulties can arise when solving such a matrix equation. Therefore the practicality of the matrix approach including experimental limitations on the input NOESY volumes was investigated. NOESY data were generated over a range of mixing times taking into account random noise, overlapping peak volumes, and the finite sensitivity for measuring cross-peak volumes by using proton coordinates from the crystal structure of lysozyme and a DNA dodecamer. A rigid molecule with a single overall correlation time was assumed. Comparison of the cross-relaxation rates, or interproton distances, obtained from the multispin matrix solution with the actual values indicates that there are errors in the matrix solution, but the errors are smaller than those obtained with the two-spin approximation under many but not all conditions of imperfect data.

### I. Introduction

The ability to determine the three-dimensional structure of proteins and nucleic acid oligomers by using interproton distances measured by NMR has been successfully demonstrated.<sup>1-6</sup> In the NMR method, interproton distances evaluated from two-dimensional nuclear Overhauser effect (NOESY) data are used as restraints in a conformational search carried out by molecular dynamics,<sup>7-9</sup> including simulated annealing protocols,<sup>10,11</sup> distance geometry,<sup>12,13</sup> or a minimization method which employs dihedral angles as independent variables.<sup>14</sup> Applications of the NMR method for structure determination have relied on obtaining a large number of distance restraints, in addition to restraints on dihedral angles and hydrogen bonds.<sup>15</sup> In most cases, interproton distances are measured approximately based on an isolated two-spin relationship for cross-relaxation<sup>16,17</sup> or only qualitatively from strong, medium, and weak NOESY cross-peak intensities.<sup>18,19</sup> Lack of quantitative distance measurements necessitates loose restraints in the conformational search; restraints are classified into distance ranges or groups, where lower bounds may be specified by van der Waals radii.<sup>17,20</sup> Although the NMR method is established, there remains a need for increasing the precision of the structures obtained.<sup>21,22</sup> One aspect of the NMR method which could

improve the structural solution is more accurate quantification of the interproton distances.

- (1) Kaptein, R.; Boelens, R.; Scheek, R. M.; van Gunsteren, W. F. *Biochemistry* **1988**, *27*, 5389-5395.
- (2) Wuthrich, K. *NMR of Proteins and Nucleic Acids*; John Wiley & Sons: New York, 1986.
- (3) Wuthrich, K. *Science* **1989**, *243*, 45-50.
- (4) Clore, G. M.; Gronenborn, A. M. *Protein Eng.* **1987**, *1*, 275-288.
- (5) Braun, W. *Q. Rev. Biophys.* **1987**, *19*, 115-157.
- (6) Wright, P. E. *TIBS* **1989**, *14*, 255-260.
- (7) Kaptein, R.; Zuiderweg, E. R. P.; Scheek, R. M.; Boelens, R.; van Gunsteren, W. F. *J. Mol. Biol.* **1985**, *182*, 179-182.
- (8) Nilsson, L.; Clore, G. M.; Gronenborn, A. M.; Brünger, A.; Karplus, M. *J. Mol. Biol.* **1986**, *188*, 455.
- (9) Clore, G. M.; Brünger, A. T.; Karplus, M.; Gronenborn, A. M. *J. Mol. Biol.* **1986**, *191*, 523-551.
- (10) Nilges, M.; Clore, G. M.; Gronenborn, A. M. *FEBS Lett.* **1988**, *229*, 317-324.
- (11) Nilges, M.; Gronenborn, A. M.; Brünger, A. T.; Clore, G. M. *Protein Eng.* **1988**, *2*, 27-38.
- (12) Pardi, A.; Hare, D. R.; Wang, C. *Proc. Natl. Acad. Sci. U.S.A.* **1988**, *85*, 8785-8789.
- (13) Havel, T. F.; Crippen, G. M.; Kuntz, I. D. *Biopolymers* **1979**, *18*, 73-81.
- (14) Braun, W.; Gö, N. *J. Mol. Biol.* **1985**, *186*, 611-626.
- (15) Nerdal, W.; Hare, D. R.; Reid, B. R. *J. Mol. Biol.* **1988**, *201*, 717-739.
- (16) Hare, D.; Shapiro, L.; Patel, D. J. *Biochemistry* **1986**, *25*, 7456-7464.
- (17) Kline, A. D.; Braun, W.; Wuthrich, K. *J. Mol. Biol.* **1988**, *204*, 675-724.

<sup>†</sup> Department of Biological Sciences.

<sup>‡</sup> Department of Chemistry.

<sup>‡</sup> Present address: Department of Medicinal Chemistry, Purdue University.